Rock and Soil Mechanics

Volume 42 | Issue 5 Article 1

9-16-2021

Experimental study and model of interface shear stress relaxation behavior of anchors in red clay

Chang-fu CHEN
College of Civil Engineering, Hunan University, Changsha, Hunan 410082, China

Cheng DU
College of Civil Engineering, Hunan University, Changsha, Hunan 410082, China

Shi-min ZHU
College of Civil Engineering, Hunan University, Changsha, Hunan 410082, China

Shi-lin HE
College of Civil Engineering, Hunan University, Changsha, Hunan 410082, China

See next page for additional authors

Custom Citation

CHEN Chang-fu, DU Cheng, ZHU Shi-min, HE Shi-lin, ZHANG Gen-bao, . Experimental study and model of interface shear stress relaxation behavior of anchors in red clay[J]. Rock and Soil Mechanics, 2021, 42(5): 1201-1209.

Experimental study and model of interface shear stress relaxation behavior of anchors in red clay

Authors

Chang-fu CHEN, Cheng DU, Shi-min ZHU, Shi-lin HE, and Gen-bao ZHANG

Rock and Soil Mechanics 2021 42(5): 1201−1209 ISSN 1000−7598
https: //doi.org/10.16285/j.rsm.2020.6429 rocksoilmech.researchcommons.org/journal

Experimental study and model of interface shear stress relaxation behavior of anchors in red clay

CHEN Chang-fu[1, 2], DU Cheng[1, 2], ZHU Shi-min[1, 2], HE Shi-lin[1, 2], ZHANG Gen-bao[3]

1. Key Laboratory of Building Safety and Energy Efficiency of Ministry of Education, Hunan University, Changsha, Hunan 410082, China
2. College of Civil Engineering, Hunan University, Changsha, Hunan 410082, China
3. College of Civil Engineering, Hunan City University, Yiyang, Hunan 413000, China

Abstract: The shear stress relaxation of the anchor-soil interface is the key factor causing the prestress loss of anchor rod (cable). Firstly, a device for testing the shear stress relaxation of the anchor-soil interface was developed. Secondly, a constant interface shear displacement was applied in stages to the red clay anchored element sample, and the whole process of shear stress relaxation curve of anchor-soil interface was obtained, which can be transformed to the relaxation curve at each specific loading level by using coordinate translation method. Then, the theory of fractional calculus was introduced to improve the viscous pot element, and established the red clay-anchor grout interface shear fractional M||N (composed of Maxwell body and Newton body in parallel) relaxation model. The model parameters were yielded by regression analysis of relaxation test curves under partial shear displacements, and the relationship between the model parameters and the shear displacements was also obtained by fitting. Finally, the established fractional M||N relaxation model was applied to predict another part of the relaxation curve under shear displacement level. By comparing the integer-order M||N model, the Burgers model and the five-element model (H||M||M), the results indicate that the proposed fractional M||N relaxation model not only has the advantages of simple structure and fewer parameters, but also has higher fitting and prediction accuracy.

Keywords: prestressed anchor; red clay; anchor-soil interface; stress relaxation; fractional calculus; M||N model

1 Introduction

The pre-stressed anchor has been widely used in the reinforcement and support of geotechnical engineering because of its strong adaptability, high cost performance, convenient construction and superior reinforcement effect. A large number of engineering practices shown that pre-stressed anchor (cable) will produce different degrees of creep and stress relaxation. The shear creep and stress relaxation at the interface between anchor and rock mass are the important factors for the creep and prestress loss of anchor (cable).

At present, many scholars have studied the shear creep characteristics of the interface between anchor and rock mass. For example, Xu et al. [1−2] carried out on-site soil grouted anchor pull-out creep tests and established a shear creep model of anchor–soil interface by using H-K model and Burgers model respectively. Kim[3] conducted creep tests and stress relaxation tests of soil grouted anchor and analyzed the creep rate and stress loss. Chen et al.[4] established an empirical creep model of anchor–soil interface based on the creep test results of anchoring element with satisfying fitting and prediction results.

In terms of the relaxation phenomenon of rock and soil mass, the scholars have performed abundant experimental research on the stress relaxation of rock and soil mass [5−12], and established various relaxation models, mainly including the empirical models[8−9] and element models [10−12]. However, the results of shear stress relaxation test and model research on the interface between anchor and rock mass have rarely been reported in literatures. Therefore, it is necessary to study the shear stress relaxation model of rock/soil mass and anchor interface in order to truly and comprehensively understand the time-dependent characteristics of soil anchor.

Most of the traditional element relaxation models are integer order models. Due to the poor adaptability and low accuracy of integer order models in describing nonlinear problems, in recent years, many scholars have introduced fractional order calculus theory[13] to establish creep models[14−17] and relaxation models[18−20] of rock and soil mass, as well as creep models of the interface between anchor and soil[21]. However, currently there is no report on the establishment of the shear stress relaxation model of anchor–rock/soil mass interface using fractional calculus theory.

In this study, a self-developed test device for the shear stress relaxation characteristics of anchor–soil interface is used to obtain the interface shear stress relaxation curves by applying constant interface shear displacements to the red clay element-scale anchoring samples. Then, the theory of fractional derivative is introduced to set up the nonlinear fractional three-element M||N (composed of Maxwell model and Newton element in parallel) relaxation model for the anchor-soil interface. Finally, the availability of the model is verified by fitting and predicting the relaxation test curves.

Received: 21 September 2020 Revised: 21 December 2020
This work was supported by the National Natural Science Foundation of China (41572298; 51978254) and the Natural Science Foundation of Hunan Province, China (2020JJ5024).
First author: CHEN Chang-fu, male, born in 1963, PhD, Professor, research interests: slope engineering, support engineering and ground treatment. E-mail: cfchen@163.com

2 Shear stress relaxation test

2.1 Test materials

The soil used in the experiment is a typical red clay from Hengyang Basin, originated from a slope excavation site in Qidong County, Hunan Province. The physical and mechanical properties of the soil are presented in Table 1, and the particle grading curve is shown in Fig.1. The uniformity coefficient and curvature coefficient of the soil used in the test are 15.0 and 1.29, respectively, with good gradation. The compression modulus of undisturbed soil is 2.77 MPa, indicating that it has strong compressibility and belongs to high compressibility soil.

Table 1 Physical and mechanical properties of test soil

Soil relative density, G_s	Liquid limit, w_L / %	Plastic limit, w_p / %	Plastic index, I_p	Optimum moisture content, w_{op} / %	Maximum dry density, $\rho_{d\,max}$ / (g • cm^{-3})	Uuniformity coefficient, C_u	Curvature coefficient, C_c	Compression modulus, E_s / MPa
2.693	57.3	33.8	23.5	25.5	1.58	15.0	1.29	2.77

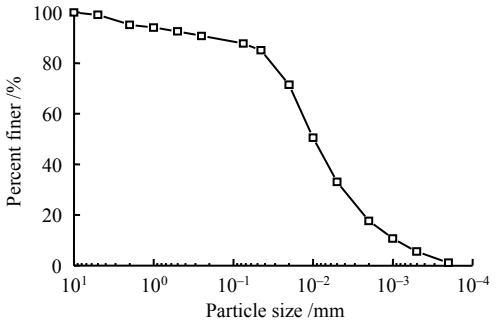

Fig. 1 Gradation curve of soil material used in the test

The cement mortar was used to fabricate the anchor grout, and the mix ratio of water: sand: cement= 0.45:1:1. The cement is P.O 42.5 ordinary Portland cement.

2.2 Test device and test method

Fig. 2 displays the self-developed test device for anchor–soil interface shear stress relaxation, including a loading system and a measuring system. The loading system is a special turbine screw lifter. The measuring system includes a force sensor, a displacement sensor and data acquisition system. Under loading, the loading handle of the turbine screw lifter is turned at a fixed rate to make the screw rod rise slowly, and then drive the force sensor and the anchor to rise in turn. The time history curve of tensile force at anchor head was measured and real-time recorded by the force sensor and the data acquisition system, respectively.

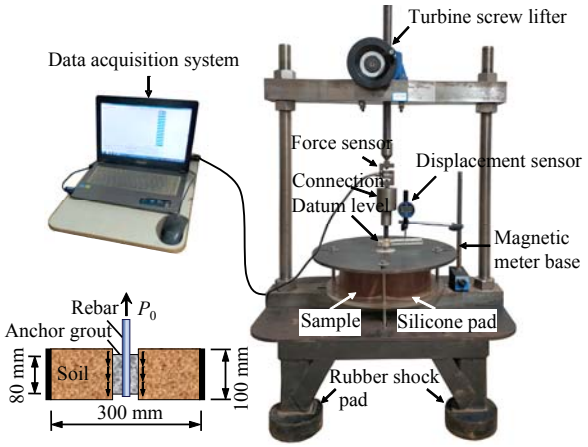

(a) Schematic diagram of test sample (b) Stress relaxation test device

Fig. 2 Anchor-soil interface shear stress relaxation test system

The samples were designed with reference to literatures [22–23]. Two groups of samples were made, and each group contained three samples, among which two were used for instantaneous pull-out test and one was used for relaxation test. The diameter and height of the sample are 300 mm and 100 mm, respectively. The length of the anchoring section is 80 mm with the diameter of the anchor hole of 48 mm. The ratio of anchor length to anchor hole diameter is $L/d = 1.67<4$, indicating that the shear stress is uniformly distributed at the anchor-soil interface, and the test results of element-scale anchoring samples could be used to simulate a micro-element in the anchoring section of the on-site anchors[24]. In addition, the ratio of sample diameter to anchor hole diameter is D/d 6.25>5, so the influence of boundary effect on the test results can be neglected[25]. The water content w and dry density ρ_d of each group were as follows: group A1, $w = 28\%$, ρ_d = 1.2 g/cm^3; group A2, $w = 28\%$, $\rho_d = 1.3$g /cm^3.

The test procedure includes soil compaction, drilling, grouting and curing, and relaxation loading. The specific steps are as follows:

(1) Soil compaction.

Pour the prepared red clay into the sample preparation mold in 5 equal parts. Under the control of dry density and layering of the compaction, the height of each layer of the compaction is 2 cm.

(2) Drilling.

Spiral dry drilling method proposed in literature [23] is adopted to drill a hole in the center of the adobe at a rate of 2 cm/min. After drilling through the compacted soil sample, the drill stem is rotated and the drill bit is pull out to obtain the anchor hole.

(3) Grouting and curing.

Firstly, place the ϕ16 mm ribbed steel bar in the center of the anchor hole. Then the prepared cement mortar is poured into the anchor hole and vibrated for compaction. After the initial setting of cement mortar, the sample is sealed and cured for 28 days.

(4) Relaxation loading.

The stress relaxation test was conducted according to a multi-stage loading method, which is divided into 5–6 steps. In each step, a constant interface shear displacement is imposed. Its value is determined according to the instantaneous pull-out test results. Under loading, the handle of the turbine screw lifter is rotated at a

fixed rate to make the screw rise slowly, and then drive the force sensor and the anchor grout which is fixed and connected by screw to rise successively. In this study, the stress relaxation stability standard is set as: the stress change value is less than 1% within continuous 24 h[5]. The preliminary test results show that for the red clay element-scale anchor- ing sample, the load applied for 5 days can reach this standard. Therefore, the loading time of each step is uniformly set to be 5 days.

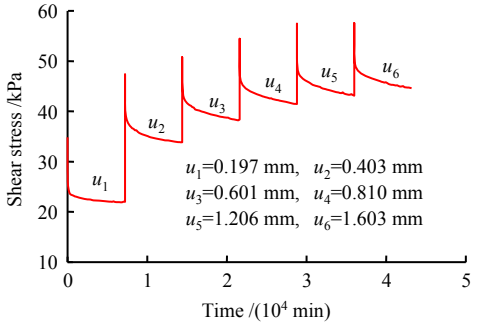

(a) Specimen A1 (w =28 %，ρ_d =1.2 g/cm³)

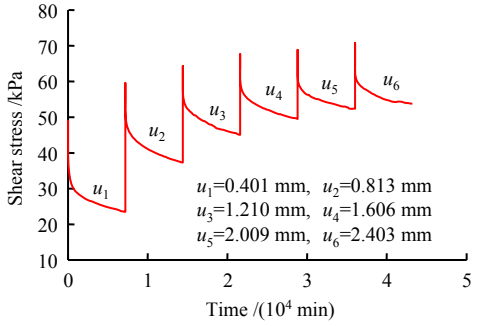

(b) Specimen A2 (w =28 %，ρ_d =1.3 g/cm³)

Fig. 3 Shear stress relaxation stepped loading curve of red clay-anchor grout interface

2.3 Test results and procedures

The whole process curves of shear stress relaxation multi-stage loading at the interface of red clay-anchor grout were obtained through relaxation tests, as shown in Fig. 3.

Creep and stress relaxation are two idealized mechanical responses of long-term mechanical properties of materials, and their microscopic mechanisms are both caused by the adjustment of geotechnical structure. In the process of creep, external energy source supplies energy to the system, while in the process of stress relaxation, there is no energy consumption of external force source, during which the stress only release due to the weakening of intergranular structure of soil [26]. For creep test, the deformation caused in later loading level includes the creep deformation formed in previous loading levels. Therefore, when do data processing, the influence of the previous loading history should be considered, and thus it is more appropriate to adopt the nonlinear "Tan's loading method"[27]. However, for relaxation test, when the constant strain is applied at each stage, the system will experience both loading and unloading stages, and the stress–strain path will form a hysteretic cycle. Compared with creep test, in stress relaxation, the load of the previous stage almost has no effect on the stress state of the specimen in the following stage. Therefore, it is more reasonable to use the "coordinate translation method" [5] to process the relaxation curve of multi-stage loading. As shown in Fig. 4, the multi-stage loading curves in Fig. 3 are converted into separate loading curves.

In Fig. 4, the shear stress at the anchor-soil interface decreases sharply at the initial stage and then gently, and eventually tends to be stable.

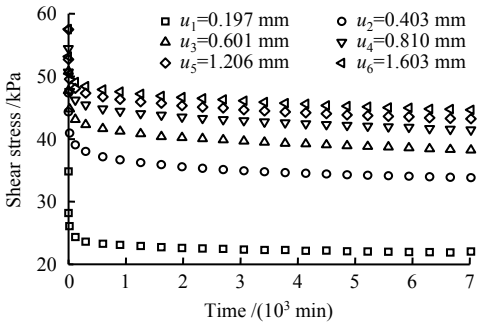

(a) Specimen A1(w =28 %，ρ_d =1.2 g/cm³)

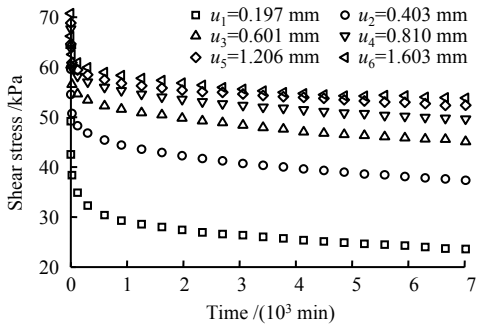

(b) Specimen A2(w =28 %，ρ_d =1.3 g/cm³)

Fig. 4 Shear relaxation separate loading curves

3 Interface shear stress relaxation model

3.1 Fractional order M||N relaxation model under individual displacement level

Fractional calculus is able to describe the time-dependent of complex mechanical process and depict the memory in time and the path dependence in space. At present, there are many definitions of fractional calculus[13]. In this paper, the widely used Riemann-Liouville fractional calculus operator theory is adopted. The fractional calculus for function $f(t)$ is defined as,

$$\frac{\mathrm{d}^{\beta} f(t)}{\mathrm{d}t^{\beta}} = {}_{t_0}D_t^{\beta} f(t) = \frac{\mathrm{d}^{n}}{\mathrm{d}t^{n}} \int_{t_0}^{t} \frac{(t-p)^{n-\beta-1}}{\Gamma(n-\beta)} f(p)\mathrm{d}p \quad (1)$$

where p is the model variable; t is time; t_0 is the initial time; β is the order of the fractional derivative, $\beta > 0$, and $n-1<\beta<n$ (n is a positive integer); ${}_{t_0}D_t^{\beta}$ is β order fractional-order calculus on $[t_0, t]$; and $\Gamma(\cdot)$ is the Gamma function, which is defined as

$$\Gamma(\beta) = \int_0^{\infty} \mathrm{e}^{-t} t^{\beta-1} \mathrm{d}t \qquad (\mathrm{Re}(\beta) > 0) \quad (2)$$

When $0 \leqslant \beta < 1$, the Laplace transform formula of Riemann-Liouville fractional calculus operator is

$$\left.\begin{aligned} L\left\{{}_0D_t^{\beta} f(t); s\right\} = s^{\beta}F(s) \\ L\left\{{}_0D_t^{-\beta} f(t); s\right\} = s^{-\beta}F(s) \end{aligned}\right\} \tag{3}$$

where s is transformation parameter; and $F(s)$ is the Laplace transformation of $f(t)$.

For soft element, based on Riemann-Liouville fractional calculus theory, its constitutive equation is

$$\tau(t) = \xi \frac{\mathrm{d}^{\beta} u(t)}{\mathrm{d}t^{\beta}} \tag{4}$$

where $\tau(t)$ is the shear stress; $u(t)$ is the displacement; ξ is a parameter similar to the viscosity coefficient of integer order, which is called viscosity-like coefficient in this study.

When $\beta = 0$, set $\xi = E$, E is the elastic modulus, then Eq. (4) describes a spring element; when $\beta = 1$, set $\xi = \eta$, η is the viscosity of coefficient, which is related to the viscosity of the material itself, then Eq.(4) describes the Newton element. In general, when $0 < \beta < 1$, the soft body element describes a viscoelastic body between an ideal Newton element and an ideal spring element, that is, soft body.

When $u(t) = \text{const.}$, it describes the relaxation of a soft body. Based on Riemann-Liouville fractional calculus theory, by applying the Laplace transform and inverse Laplace transform to Eq. (4), the relaxation equation of soft body element can be expressed as

$$\tau(t) = \xi \frac{t^{-\beta}}{\Gamma(1-\beta)} u \tag{5}$$

where u is displacement.

Based on the parallel Maxwell model and Newton element (i.e., M||N model), fractional order calculus theory is introduced to improve the dashpot element, a three-element fractional order M||N shear stress relaxation model for red clay–anchor grout interface is established, as illustrated in Fig. 5.

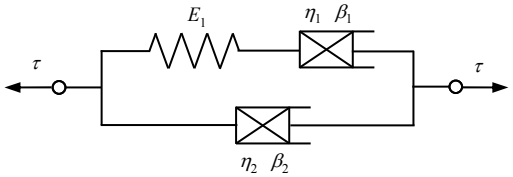

Fig. 5 Fractional M||N relaxation model

$$\tau = \tau_{\mathrm{M}} + \tau_{\mathrm{N}}, \quad u = u_{\mathrm{M}} = u_{\mathrm{N}} \tag{6}$$

$$\tau_{\mathrm{M}} = \frac{E_1\eta_1 D_1}{E_1 + \eta_1 D_1} u_{\mathrm{M}}, \quad \tau_{\mathrm{N}} = \eta_2 D_2 u_{\mathrm{N}} \tag{7}$$

where τ is the shear stress; τ_{M} and u_{M} are the stress and displacement of fractional order Maxwell model, respectively; τ_{N} and u_{N} are the stress and displacement of fractional soft body element, respectively; E_1 is the elastic modulus of spring element; η_1 and η_2 are viscosity-like coefficients; D_1 and D_2 are fractional operators, $D_1 = \dfrac{\mathrm{d}^{\beta_1}}{\mathrm{d}t^{\beta_1}}$, $D_2 = \dfrac{\mathrm{d}^{\beta_2}}{\mathrm{d}t^{\beta_2}}$; and β_1 and β_2 are fractional differential orders.

By combining the Eqs. (6) and (7), the fractional constitutive model can be obtained as,

$$\tau = \left(\frac{E_1\eta_1 D_1}{E_1 + \eta_1 D_1} + \eta_2 D_2\right) u \tag{8}$$

Take the Laplace transform of Eq. (8), set $u(t) = u_0 H(t)$, $H(t)$ is Heaviside unit step function, thus the shear stress is expressed as

$$\tau = L^{-1}\left[\left(\frac{E_1\eta_1 s^{\beta_1}}{E_1 + \eta_1 s^{\beta_1}} + \eta_2 s^{\beta_2}\right)\frac{u_0}{s}\right] \tag{9}$$

where u_0 is the initial displacement, which is equal to the applied displacement at $t = 0$, $u_0 = u(t)\big|_{t=0}$ is a constant value during stress relaxation, and therefore the stress relaxation equation is obtained as,

$$\tau(t) = G(t) \cdot u_0 \tag{10}$$

where $G(t)$ is the relaxation modulus. According to Eq. (9), the Laplace transform of relaxation modulus can be written as

$$\begin{aligned} G(t) = L^{-1}\left[\left(\frac{E_1\eta_1 s^{\beta_1}}{E_1 + \eta_1 s^{\beta_1}} + \eta_2 s^{\beta_2}\right)\frac{1}{s}\right] = \\ L^{-1}\left[E_1 \frac{\eta_1 s^{\beta_1 - 1}}{s^{\beta_1} + \dfrac{E_1}{\eta_1}} + \eta_2 s^{\beta_2 - 1}\right] \end{aligned} \tag{11}$$

In order to obtain the inverse Laplace transform of Eq. (11), the Mittag-Leffler (M-L) function is introduced into the first term of Eq. (11), and then perform the Laplace transform and the inverse transform directly for the second term. The generalized M-L function is defined as follows [13]:

$$E_{\alpha,\gamma}(z) = \sum_{k=0}^{\infty} \frac{z^k}{\Gamma(\alpha k + \gamma)} \quad (\alpha, \gamma > 0; z \in C) \tag{12}$$

where α, γ, k are the model parameters; z is the independent variable and C is a complex set.

The Laplace transform of the M-L function is

$$\int_0^{\infty} \mathrm{e}^{-st} t^{\alpha k + \gamma - 1} E_{\alpha,\gamma}^{(k)}(\pm n t^{\alpha}) \mathrm{d}t = \frac{k!\, s^{\alpha - \gamma}}{(s^{\alpha} \mp n)^{k+1}} \quad (\mathrm{Re}(s) > |n|^{\frac{1}{\alpha}}) \tag{13}$$

where $E_{\alpha,\gamma}^{(k)}(z)=\dfrac{\mathrm{d}^k}{\mathrm{d}z^k}E_{\alpha,\gamma}(z)$.

By comparing Eq. (11) with Eq. (13), it can be seen that when parameters in the first term of Eq. (13) are set as $k=0$, $\gamma=1$, and $\alpha=\beta_1$, $n=E_1/\eta_1$, the obtained relaxation modulus is

$$G(t)=E_1E_{\beta_1,1}\left(-\frac{E_1}{\eta_1}t^{\beta_1}\right)+\eta_2\frac{t^{-\beta_2}}{\Gamma(1-\beta_2)} \tag{14}$$

Consequently, the shear stress relaxation equation of the anchor–soil interface is derived as

$$\tau(t)=G(t)u_0=\left[E_1E_{\beta_1,1}\left(-\frac{E_1}{\eta_1}t^{\beta_1}\right)+\eta_2\frac{t^{-\beta_2}}{\Gamma(1-\beta_2)}\right]u_0 \tag{15}$$

It is worth noting that in Eq. (15), the elastic modulus E_1, coefficients of viscosity η_1, η_2, fractional differential order β_1 and β_2 are five model parameters, and their values can be obtained by regression analysis of test results.

3.2 Fractional M||N relaxation model considering the effects of displacement level

Equation (15) is the proposed relaxation model at different displacement levels, and the model parameters E_1, η_1, β_1, η_2 and β_2 change with the applied displacement $u_i(i=1,2,\cdots,6)$. Therefore, these model parameters are the functions of displacement u.

According to the variation characteristics of the instantaneous pull-out curve, it is found that the shear stiffness and displacement of the interface show an exponential trend. Meanwhile, the shear stress relaxation curves of red clay–anchor interface are fitted and the results show that in Eq. (15), the elastic modulus E_1, coefficient of viscosity η_1, coefficient of viscosity η_2 and fractional differential order β_1 change exponentially with the applied displacement u, while the fractional differential order β_2 basically remains unchanged, which can be considered as a constant and can be represented by a mean value. In addition, when the displacement level of each stage is applied, the shear stress at the soil–anchor interface corresponding to the applied displacement reaching the set value is defined as the initial shear stress $\tau_0=\tau(t)\big|_{t=0}$, which changes exponentially with the applied displacement level. In this way, the red clay–anchor interface shear fractional M||N model considering the influences of displacement level is established as follow:

$$\left.\begin{aligned}
&\tau(t)=\left[E_1E_{\beta_1,1}\left(-\frac{E_1}{\eta_1}t^{\beta_1}\right)+\eta_2\frac{t^{-\beta_2}}{\Gamma(1-\beta_2)}\right]u\\
&E_1=a_{E_1}\exp(b_{E_1}u)+c_{E_1}\\
&\eta_1=a_{\eta_1}\exp(b_{\eta_1}u)+c_{\eta_1}\\
&\beta_1=a_{\beta_1}\exp(b_{\beta_1}u)+c_{\beta_1}\\
&\eta_2=a_{\eta_2}\exp(b_{\eta_2}u)+c_{\eta_2}\\
&\beta_2=\text{const.}
\end{aligned}\right\} \tag{16}$$

where a_{E_1}, b_{E_1}, c_{E_1}, a_{η_1}, b_{η_1}, c_{η_1}, a_{β_1}, b_{β_1}, c_{β_1}, a_{η_2}, b_{η_2}, c_{η_2} and β_2 are the coefficients determined by analysis of test results.

3.3 Parameters determination

The results of sample A1 in Section 2.3 (Fig. 4(a)) are taken as an example to illustrate the process of parameters determination and model establishment.

(1) As shown in Fig. 6, Eq. (15) is used to fit the relaxation curves at all displacement levels $u_i(i=1,2,\cdots,6)$ presented in Fig. 4(a). Thus, the corresponding model parameter values and correlation coefficients R^2 are obtained, as summarized in Table 2. It shows good fitting results for the proposed model.

(2) Next, the change relationships between model parameters E_1, η_1, β_1, η_2, β_2 and applied displacement u are plotted in Fig. 7. By regression analysis, the empirical formulas for the changes of model parameters with displacement u are derived. And the red clay–anchor interface shear stress relaxation model of sample A1 is obtained as follows:

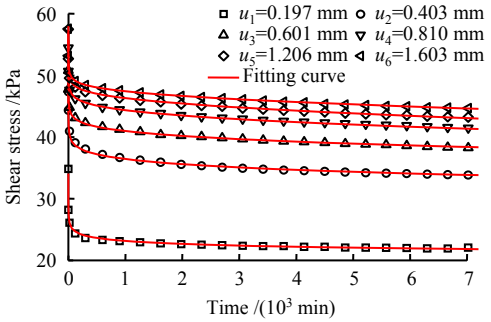

Fig. 6 Fitting effect of fractional M||N model on specimen A1

Table 2 Fitting results of relaxation curve of A1 sample based on fractional M||N model

u / mm	τ_0 / kPa	E_1 / (kPa • mm^{-1})	η_1 / (kPa • min • mm^{-1})	β_1	η_2 / (kPa • min • mm^{-1})	β_2	R^2
0.197	34.830	99.24	4 337.5	0.159	53.22	0.10	0.987
0.403	47.344	81.92	17 546.2	0.351	27.91	0.10	0.991
0.601	50.805	61.56	50 824.2	0.464	18.38	0.10	0.990
0.810	54.450	49.96	76 404.2	0.539	13.39	0.10	0.992
1.206	57.466	35.05	144 980.0	0.648	8.87	0.10	0.991
1.603	57.557	26.94	218 729.9	0.694	6.55	0.10	0.995

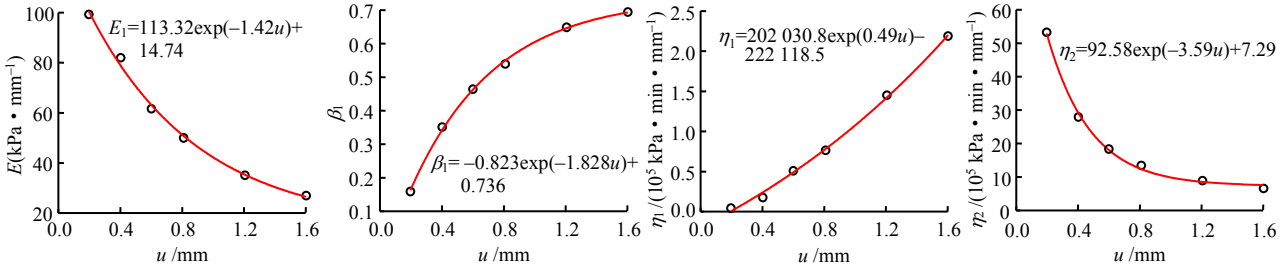

(a) E_1 Parameters fitting (b) β_1 Parameters fitting (c) η_1 Parameters fitting (d) η_2 Parameters fitting

Fig. 7 Relationships between relaxation model parameters of A1 sample and interface shear displacement u

$$\left.\begin{aligned}
&\tau(t)=\left[E_1E_{\beta_1,1}\left(-\frac{E_1}{\eta_1}t^{\beta_1}\right)+\eta_2\frac{t^{-\beta_2}}{\Gamma(1-\beta_2)}\right]u\\
&E_1=113.32\exp(-1.42u)+14.74\\
&\eta_1=202\ 030.8\exp(0.49u)-222\ 118.5\\
&\beta_1=-0.823\exp(-1.828u)+0.736\\
&\eta_2=92.58\exp(-3.59u)+7.29\\
&\beta_2=0.10
\end{aligned}\right\}\qquad(17)$$

According to the above modeling methods and procedures, the relaxation curves corresponding to u_1, u_2, u_4 and u_6 in sample A2 is modeled by regression (Fig. 4(b)), and the shear stress relaxation model of red clay–anchor interface of sample A2 can be obtained:

$$\left.\begin{aligned}
&\tau(t)=\left[E_1E_{\beta_1,1}\left(-\frac{E_1}{\eta_1}t^{\beta_1}\right)+\eta_2\frac{t^{-\beta_2}}{\Gamma(1-\beta_2)}\right]u\\
&E_1=120.18\exp(-1.48u)+20.33\\
&\eta_1=37\ 368.1\exp(0.54u)-44\ 995.0\\
&\beta_1=-0.586\exp(-0.880u)+0.739\\
&\eta_2=41.25\exp(-1.89u)+5.04\\
&\beta_2=0.10
\end{aligned}\right\}\qquad(18)$$

The fitting results are presented in Fig. 8 with model parameter values and correlation coefficients R^2 showing in Table 3.

4 Comparative analysis of fractional order model and integer order model

The fractional model proposed in this study is compared with several integer order models to verify the rationality and reliability of our new model. Integer order models include the corresponding integer order M||N model, Burgers model, five-element model (H||M||M) in literature [18].

4.1 Fitting results analysis

Similarly, the sample A2 in Section 2.3 (Fig. 4(b)) is analyzed as an example. The relaxation curves corresponding to the applied displacements u_1, u_2, u_4 and u_6 are selected for regression modeling. The relaxation curves corresponding to u_3 and u_5 are used for prediction and comparative analysis. According to the modeling methods and procedures described in Section 3.3, the red clay–anchor interface shear stress relaxation model of integer order M||N model, Burgers model and five-element model (H||M||M), the fitting curves, the parameter values and the correlation coefficient R^2 can all be obtained. Due to the limited paper length, only the fitting curves are presented here, as shown in Fig. 9.

As can be observed in Fig. 9, from integer order M||N model, Burgers model, five-element model, to our new fractional model, the fitting accuracy is gradually getting better. Although the fitting correlation coefficient R^2 of five-element model is relatively high, there is still a certain deviation between the fitting curve and the experimental value, especially at the initial and inflection point. In addition, at the low shear displacement level, the fitting performance of the five-element model is not as good as that of the proposed fractional model.

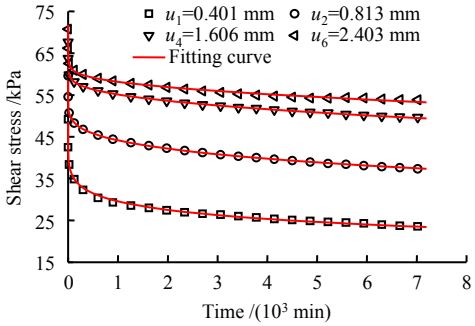

Fig. 8 Fitting effect of fractional M||N model on specimen A2

Table 3 Fitting results of relaxation curve of specimen A2 based on fractional M||N model

u / mm	τ_0 / kPa	E_1 / (kPa • mm^{-1})	η_1 / (kPa • min • mm^{-1})	β_1	η_2 / (kPa • min • mm^{-1})	β_2	R^2
0.401	49.166	87.64	2 338.8	0.324	24.38	0.10	0.995
0.813	59.569	54.71	11 924.4	0.461	13.83	0.10	1.000
1.606	67.631	32.48	43 149.6	0.587	7.16	0.10	0.998
2.403	70.740	22.29	91 104.3	0.673	5.39	0.10	0.992

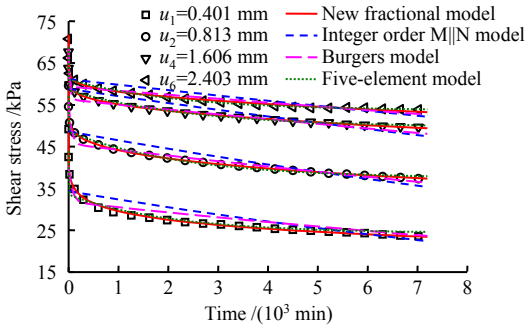

Fig. 9 Model fitting of specimen A2

In order to quantitatively describe the superiority of the nonlinear relaxation model in reflecting the shear stress relaxation characteristics of red clay– anchor interface, Table 4 presents the mean square error (RMSE) and correlation coefficient R^2 of the measured results in the fitting of the displacement levels u_1, u_2, u_4 and u_6 in sample A2 as quantitative evaluation indexes.

It is clear in Table 4, with the minimum RMSE and maximum R^2, nonlinear relaxation model fitting effect is superior to the integer order M||N model, Burgers model and five-element model. The analysis reveals that the fractional model presented in this paper is simpler and accurately reflect the whole process of shear stress relaxation at red clay–anchor interface.

Table 4 Evaluation of model fitting accuracy

Relaxation model	Mean square error RMSE				Correlation coefficient R^2			
	u_1	u_2	u_4	u_6	u_1	u_2	u_4	u_6
Fractional model	0.413	0.539	0.175	0.360	0.995	0.989	0.998	0.992
Integer order M||N model	3.747	2.635	2.219	2.317	0.629	0.744	0.723	0.655
Burgers model	2.044	0.965	0.960	0.875	0.937	0.966	0.964	0.950
Five-element model	1.369	0.636	0.465	0.498	0.973	0.985	0.988	0.986

4.2 Model prediction analysis

The relaxation curves corresponding to sample A2 interfacial shear displacement levels of u_1, u_2, u_4 and u_6 in Section 2.3 are analyzed via regression. The relaxation models corresponding to fractional model, integer order M||N model, Burgers model and five-element model are obtained successively. Furthermore, the relaxation curves under interface shear displacements of u_3 and u_5 are predicted. The results are plotted in Fig.10. Meanwhile, error analysis is carried out on the prediction of u_3 and u_5 in sample A2, and the results are listed in Table 5.

Figure 10 clearly demonstrates that the prediction effect of the proposed fractional relaxation model is the best, followed by five-element model. The Burgers model and integer order M||N model have worse fitting accuracy. Five-element model, although has similar predictions, is more complex compared with fractional model. In addition, the minimum RMSE and maximum R^2 of the prediction results of the fractional model further indicate that the fractional model proposed in this paper is better than other models. According to the above analysis, the shear stress relaxation model of red clay–anchor interface established in this study not only has a good fitting accuracy, but also exhibits a strong predictive capability.

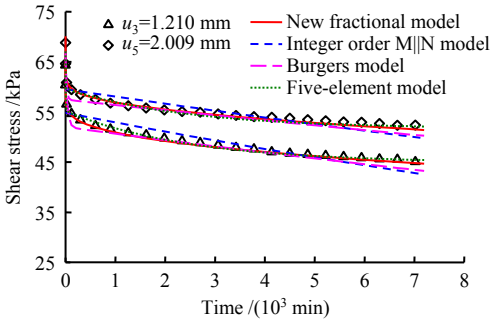

Fig. 10 Model prediction of specimen A2

Table 5 Error analysis of model prediction results

Relaxation model	Mean square error RMSE		Correlation coefficient R^2	
	u_3	u_5	u_3	u_5
Fractional model	0.457	0.490	0.990	0.983
Integer order M||N model	2.340	2.250	0.750	0.665
Burgers model	1.171	1.160	0.966	0.958
Five-element model	0.536	0.613	0.987	0.982

5 Conclusions

(1) In order to study the shear stress relaxation characteristics of anchor interface in red clay, a test device for shear stress relaxation of anchor–soil interface was developed independently. For the red clay element-scale anchoring samples, the constant interface shear displacements were applied using a multi-stage loading method, and the whole process of interface shear stress relaxation curve was then obtained.

(2) Based on the fractional calculus theory, a new model of shear stress relaxation at the interface of red clay–anchor was established by introducing a soft body element between an ideal Newton element and an ideal spring element to replace the traditional Newton element. The proposed fractional M||N relaxation model is not only simple, but also can accurately fit and predict the shear stress relaxation behavior at the anchor–soil interface under different displacement levels.

(3) By comparing the model fitting and prediction results of integer order M||N model, Burgers model and five-element model (H||M||M) and fractional M||N model, it is found the proposed three-element fractional M||N relaxation model has the advantages of fewer parameters, higher accuracy, and easy to be applied in practical engineering in describing the shear stress relaxation characteristics of anchor–soil interface. This research provides a theoretical basis for the analysis of stress relaxation behavior of grouted anchors installed in red clay under long-term load.

References

[1] XU Hong-fa, LU Hong-biao, QIAN Qi-hu. Creep damage effects of pulling grouting anchor in soil[J]. Chinese Journal of Geotechnical Engineering, 2002, 24(1): 61–63.

[2] XU Hong-fa, SUN Yuan, CHEN Ying-cai. Study on creep tests of soil anchors[J]. Journal of Geotechnical Investigation & Surveying, 2006, (9): 6–8, 53.

[3] KIM N K. Performance of tension and compression anchors in weathered soil[J]. Journal of Geotechnical and Geoenvironmental Engineering, 2003, 129(12): 1138–1150.

[4] CHEN Chang-fu, LIU Jun-bin, XU You-lin, et al. Tests on shearing creep of anchor-soil interface and its empirical model[J]. Chinese Journal of Geotechnical Engineering, 2016, 38(10): 1762–1768.

[5] SUN Jun. Rheological behavior of geomaterials and its engineering applications[M]. Beijing: China Architecture and Building Press, 1999.

[6] SCHULZE O. Strengthening and stress relaxation of Opalinus clay[J]. Physics and Chemistry of the Earth, 2011, 36(17-18): 1891–1897.

[7] WANG Z, GU L L, SHEN M R, et al. Shear stress relaxation behavior of rock discontinuities with different joint roughness coefficients and stress histories[J]. Journal of Structural Geology, 2019, 126: 272–285.

[8] WANG Zhi-jian, YIN Kun-long, JIAN Wen-xing, et al. Experimental study on soil relaxation in Anlesi landslide zone of Wanzhou[J]. Chinese Journal of Rock Mechanics and Engineering, 2008, 27(5): 931–931.

[9] XIONG Liang-xiao, YANG Lin-de, ZHANG Yao. Stress relaxation tests on green schist specimens under multi-axial compression[J]. Chinese Journal of Geotechnical Engineering, 2010, 32(8): 1158–1165.

[10] TIAN Hong-ming, CHEN Wei-zhong, XIAO Zheng-long, et al. Experimental study on triaxial compression relaxation of argillaceous siltstone with high confining pressure[J]. Chinese Journal of Geotechnical Engineering, 2015, 37(8): 1433–1439.

[11] ZHAO Zhen-hua, ZHANG Xiao-jun, LI Xiao-cheng. Experimental study of stress relaxation characteristics of hard rocks with pressure relief hole[J]. Rock and Soil Mechanics, 2019, 40(6): 2192–2199.

[12] YU H C, ZHANG X S, LIU H D, et al. Stress relaxation behavior of silty mudstone considering the effect of confining pressure[J]. Environmental Earth Sciences, 2016, 75(12): 1001.

[13] CHEN Wen. Fractional derivative modeling of mechanical and engineering problems[M]. Beijing: Science Press, 2010.

[14] LIU Jia-shun, JING Hong-wen, MENG Bo, et al. Research on the effect of moisture content on the creep behavior of weakly cemented soft rock and its fractional-order model[J]. Rock and Soil Mechanics, 2020, 41(8): 2609–2618.

[15] WU F, LIU J F, WANG J. An improved Maxwell creep model for rock based on variable-order fractional derivatives[J]. Environmental Earth Sciences, 2015, 73(11): 6965–6971.

[16] ZHOU H W, WANG C P, HAN B B, et al. A creep constitutive model for salt rock based on fractional derivatives[J]. International Journal of Rock Mech- anics and Mining Sciences, 2011, 48(1): 116–121.

[17] LUO Qing-zi, CHEN Xiao-ping, WANG Sheng, et al. Experimental and empirical model research on deformation timeliness of soft clay[J]. Rock and Soil Mechanics, 2016, 37(1): 66–75.

[18] YU Huai-chang, SHI Guang-cheng, LIU Han-dong, et al. Study on nonlinear viscoelastic stress relaxation model of rock based on fractional order calculus[J]. Journal of Applied Foundation and Engineering Science, 2019, 27(1): 194–204.

[19] ZHANG Chun-xiao, XIAO Hong-bin, BAO Jia-miao, et al. Fractional order model of stress relaxation in expansive soil[J]. Rock and Soil Mechanics, 2018, 39(5): 1747–1752.

[20] WANG Ming-wu, XU Xin-yu, ZHOU Tian-long, et al. The fractional order relaxation model of net-like red soil[J]. Chinese Journal of Computational Mechanics, 2020, 37(3): 362–367.

[21] CHEN Chang-fu, GAO Jie, LIU Jun-bin, et al. A factional-derivative-based creep model for the soil-anchor interface in the anchored slope with the soil expanding[J]. Journal of Safety and Environment, 2018, 18(5): 1847–1854.

[22] CHEN Chang-fu, LIANG Guan-ting, TANG Yu, et al. Anchoring solid-soil interface behavior using a novel laboratory testing technique[J]. Chinese Journal of Geotechnical Engineering, 2015, 37(6): 1115–1122.

[23] WEN Yong-kai, CHEN Chang-fu, ZHU Shi-min, et al. Experimental investigation on grout-soil interface shear behavior for grouted anchor in red clays based on drilled element anchor specimens[J]. China Science Paper, 2020, 15(8): 855–861.

[24] BENMOKRANE B, CHENNOUF A, MITRI H S. Laboratory evaluation of cement-based grouts and grouted rock anchors[J]. International Journal of Rock Mechanics and Mining Sciences & Geomechanics Abstracts, 1995, 32(7): 633–642.

[25] COOKE R W, PRICE G, TARR K. Jacked piles in London clay: a study of load transfer and settlement under working conditions[J]. Géotechnique, 1979, 29(2): 113–147.

[26] LI Jun-shi. Numerical discussion creep and stress on coupled effects of relaxation of clay[J]. Rock and Soil Mechanics, 2001, 22(3): 294–297.

[27] TAN T K, KANG W F. Locked in stresses, creep and dilatancy of rocks, and constitutive equations[J]. Rock Mechanics, 1980, 13(1): 5–22.